PCCP

COMMUNICATION

View Article Online
View Journal | View Issue

Cite this: *Phys. Chem. Chem. Phys.*, 2017, **19**, 21276

Received 19th April 2017,
Accepted 21st July 2017

DOI: 10.1039/c7cp02550e

rsc.li/pccp

Does the endohedral borospherene supersalt $FLi_2@B_{39}$ maintain the "super" properties of its subunits?†

A. J. Stasyuk * and M. Solà *

The behavior of the entirely unique system represented by superalkaline species incorporated into a superhalogen cage has been studied using density functional theory with hybrid functionals and the triple-ξ quality basis set level of theory. The singlet ground state and triplet excited state of an $FLi_2@B_{39}$ borospherene complex as well as its cationic and anionic doublet ground states have been investigated. Only the encapsulation of FLi_2^+ into B_{39} in $FLi_2@B_{39}^+$ is a thermodynamically unfavorable process. All other systems are stabilized during encapsulation most likely *via* an unpaired electron delocalization process and electrostatic interaction. The calculations revealed that superhalogen and superalkaline properties inherent in the separated fragments are lost in $FLi_2@B_{39}$ complexes. The applicability of vertically estimated ionization potentials and electron affinities instead of adiabatic ones for description of such systems has been demonstrated.

In the early 80s, Gutsev and Boldyrev demonstrated the existence of two classes of extraordinary molecular systems, the so-called superalkalis (SAs)[1,2] and superhalogens (SHs).[3,4] Superalkalis are molecules or clusters possessing lower ionization potentials (IPs) than those of alkali metals (5.39–3.89 eV),[5] while superhalogens are polyatomic systems featured by electron affinities (EAs) that may exceed 3.61 eV, *i.e.* the limit of chlorine.[5] Later in the early 90's, the general superatom concept was formulated.[6–10] During the past three decades the interest of scientists throughout the world in this phenomenon has been continuously increasing. A lot of theoretical[11–15] and experimental[16–19] studies have been carried out to elucidate the structural and electronic properties of these systems.

Most of the investigated SA clusters belong to the empirical formula of $XM_{(n+k)}$, where n is the maximal formal valence of electronegative atom X, $k \geq 1$ and M is an electropositive/metal element. The first experimentally discovered SA was OLi_3, observed by Wu *et al.* in 1979.[17,20] A few years later, Schleyer *et al.* discovered theoretically a large number of XM_n molecules composed of first-row elements with unusual stoichiometries. Despite the fact that in these systems violations of the octet rule were observed, they show thermodynamic stability toward dissociation or loss of an electron.[21] A variety of interesting SAs with one non-metallic center species have been intensively studied both theoretically and experimentally.[22–27] No less attention was paid to SHs. Molecules with high EA usually act as strong oxidizing agents that can react with various groups of chemical compounds while they themselves tend to form very stable negatively charged ions. Traditional SHs are usually represented by a simple formula – $MX_{(n+k)}$, where M is the central atom with maximal formal valence n, $k \geq 1$ and X is a halogen atom. Due to the high application potential of SHs in the synthesis of new chemical compounds,[27–30] and nonlinear optical[31,32] and magnetic materials,[33–36] substantial efforts have been made towards their theoretical and experimental investigation. Recent studies have demonstrated the applicability of SHs in new halogen-free Li-ion batteries[37,38] and the possibility of SHs serving as dopants for tuning electronic and magnetic properties. Furthermore, in the last few years researchers have demonstrated that clusters containing no halogen or metal atoms can exhibit SH properties.[39–41]

The most exciting discovery of recent years in the chemistry of SH materials was connected with the discovery of all-boron fullerenes D_{2d} B_{40}^- and B_{40}^0 (referred to in the literature as borospherenes).[42] Right after that, the B_{39}^- nanocluster with C_3 symmetry,[43] which was produced *via* laser vaporization of a ^{10}B-enriched boron target, was discovered. Two other cationic borospherenes C_1 B_{41}^+ and C_2 B_{42}^{2+} were found by Chen *et al.* on the basis of global minimum structural searches.[44] In addition, a significant number of studies devoted to the electronic structures and spectral properties of various borospherenes have been published.[39,45–47] Photoelectron spectroscopy of C_3–B_{39}^- detects leading bands with a vertical detachment energy of 4.00(5) eV.

Institut de Química Computacional and Departament de Química, Universitat de Girona, C/ Maria Aurèlia Capmany 69, 17003 Girona, Catalonia, Spain. E-mail: anton.stasyuk@udg.edu, miquel.sola@udg.edu

† Electronic supplementary information (ESI) available: Full computational details, Tables S1–S6 containing ionization potentials, electron affinities, geometrical parameters for Li_2F at different levels of theory, encapsulation energies, and charges and spin densities together with Cartesian coordinates of all optimized species. See DOI: 10.1039/c7cp02550e

Based on this, an adiabatic detachment energy of 3.84(5) eV that represents the EA of neutral B_{39}^0 was determined. This in turn allows the classification of B_{39}^0 species as SHs.[43] Similar to a C_{60} buckyball,[48–50] immediately after the discovery of the borospherenes, a family of endohedral metalloborospherenes $M@B_{40}$ was predicted by Bai *et al.*[51,52] Recently, Chen *et al.* have foreseen the first axially chiral endohedral $Ca@B_{39}^+$ monocation.[53] Besides that, the stabilization of B_{37}^{3-} trianion[54] and B_{38}^{2-} dianion[55] borospherenes by metal encapsulation has been reported. Also it has been shown that lithium-decorated borospherene B_{40} could be a promising medium for hydrogen storage.[56] Particularly, the recent work published by Misra *et al.* should be mentioned, where the authors demonstrated that SAs encapsulated into C_{60} fullerenes are thermodynamically stable.[57]

The ability of borospherenes to act as hosts for various alkaline/alkaline-earth and transition metals has been clearly demonstrated. It is well-known that fullerene C_{60} could host small molecules, like H_2,[58,59] H_2O[59–61] or HF.[62] Based on the similarity of the molecular diameters of buckminsterfullerene and borospherene B_{39} we assumed that a B_{39} cage could host not just metal cations but also small molecules. In cases where the encapsulated molecule can demonstrate superalkaline properties, we would have an entirely unique system representing superalkaline species incorporated into a superhalogen cage. In this work we report a systematic computational study of endohedral C_3–B_{39} borospherene (constitute SH) containing SA FLi_2 species.

There are multiple studies devoted to the structural and electronic properties of clusters formed by SH and SA subunits. Such supersalts (SSs) are characterized by significant non-linear properties and demonstrate preferential ionic dissociation pathways.[63–65] It has to be mentioned that until now all studied SSs are described as two-dimensional structures in which one subunit is allocated near another. Discovery of the B_{39} cage SH allowed the construction of a SS in which the SA subunit is situated inside the SH subunit. Taking into account the fact that B_{39}^- borospherene possesses a cavity with a diameter close to 6.0 Å, the SA subunit selection was primarily made based on its spatial size. One of the smallest known SA species is hypervalent FLi_2. The ionization energy detected by electron impact mass spectrometry using a surface ionization method was 3.78 ± 0.2 eV for FLi_2.[66,67] The experimentally determined ionization energy as well as *ab initio* MO calculations confirmed that the FLi_2 species takes a SA configuration in which the odd-electron is delocalized over lithium atoms.[27,68]

In the work by Wang and co-workers[43] on axially chiral B_{39}^- borospherene the authors used PBE0 and CAM-B3LYP functionals furnished with the 6-311+G(d) basis set for the optimization of low-lying isomers. The most stable C_3–B_{39}^- isomer found in that study has been chosen as the starting point for our project.

In our work, B3LYP and PBE0 functionals with double- and triple-ξ quality basis sets have been tested for both FLi_2 and B_{39} species in neutral and charged forms (Table S1, ESI†). Based on the benchmark results it should be noted that the performance of both studied functionals is comparable with a slight advantage of the PBE0 functional. At the same time, the effect of the basis set size in each case was not significant. The latter circumstance has allowed us to use a 6-31+G(d) basis set for preliminary calculations. However, the final supermolecules formed by B_{39} and FLi_2 subunits were fully optimized and their relative energies were evaluated with the 6-311+G(2d) basis set (see the ESI† for the detailed computational procedure).

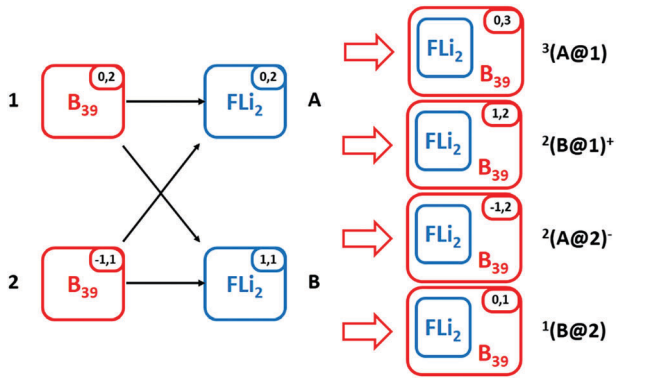

Fig. 1 The studied endohedral supermolecules with total charge and multiplicity constructed from $B_{39}^{0/1-}$ and $FLi_2^{0/1+}$ subunits.

Taking into account that each of two subunits could exist in two forms – SH or SA and their conjugated ions, we could construct four supermolecules (Fig. 1).

Supermolecules ^{2}(B@1)$^+$ and ^{2}(A@2)$^-$ represent cationic and anionic doublets, respectively. ^{3}(A@1) is a neutral triplet structure formed by merging the SA and SH, while ^{1}(B@2) is a neutral singlet built from SA cations and SH anions. The ^{1}(B@2) structure could be assigned as an actual supersalt. ^{1}(B@2) could also be denoted as ^{1}(A@1) and considered to be formed by SA and SH fragments. However, the electronic structure of singlet $LiF_2@B_{39}$ is closer to $LiF_2^+@B_{39}^-$ (see Table S6, ESI†) and, for this reason, we prefer to name it by considering it as being built from SA cations and SH anions, *i.e.*, ^{1}(B@2).

Considering the rather small B_{39} cavity size, it seems likely that rotation of the FLi_2 fragment is limited, which in turn implies the existence of several conformers with different relative fragment orientations with respect to each other. For verification of this hypothesis, we generated 12 starting geometries for the ^{1}(B@2) system different in terms of the orientation of the FLi_2 fragment (Fig. S1, ESI†). An unconstrained optimization procedure for the above-mentioned 12 initial geometries revealed 4 unique conformers of the ^{1}(B@2) supermolecule. Graphical representations and relative energies of the found conformers are depicted in Fig. 2.

The found conformers are significantly different in energy, such that all conformers are located in a 18.5 kcal mol^{-1} range. For all other studied supermolecules (^{3}(A@1), ^{2}(B@1)$^+$ and ^{2}(A@2)$^-$) a similar procedure has been performed. The relative stability for the found conformers is displayed in Fig. S2, ESI.†

At the next stage of our work we optimized the neutral singlet and triplet as well as cationic and anionic electronic states of the $FLi_2@B_{39}$ supermolecule with both PBE0 and B3LYP functionals equipped with the 6-31+G(d) basis set. To evaluate the stability of

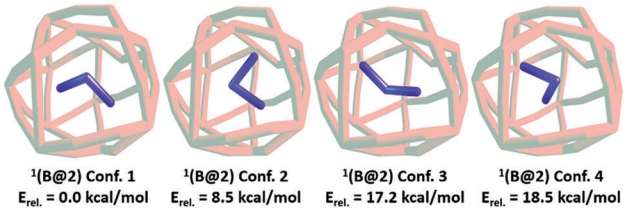

Fig. 2 Graphical representation and relative energies of ^{1}(B@2) conformers obtained at the PBE0/6-31+G(d) level of theory.

the designed supermolecules, encapsulation energies have been estimated. Surprisingly, we have found that PBE0 and B3LYP functionals provide qualitatively different results (Table S3, ESI†). The results obtained with the PBE0 functional indicate that formation of ^{3}(A@1) and ^{2}(A@2)$^-$ supermolecules is energetically a favorable process accompanied by the release of *ca.* 14 kcal mol^{-1}. At the same time, B3LYP results demonstrate that the denoted encapsulation reactions are endothermic. In order to get a more convincing answer to the question of whether the encapsulation is an endothermic or exothermic process we tried other hybrid functionals such as TPSSh,[69,70] mPW1PW91[71] and HSEH1PBE (in the literature known as HSE06)[72,73] (Table S3, ESI†). The results obtained with the "new" functionals clearly support the results produced with the PBE0 functional. However, in order to be absolutely sure of the correctness of the choice, the encapsulation energy for the ^{1}(B@2) complex on the basis of CCSD(T) calculations (DLPNO-CCSD(T)) has been determined. Analysis of the equilibrium geometries for each of the studied supermolecules ^{3}(A@1), ^{2}(B@1)$^+$ and ^{2}(A@2)$^-$ obtained with different hybrid functionals revealed minimal differences in geometrical parameters (RMSD values lie in the range from 0.003 to 0.027, Table S4, ESI†). Thus it can be argued that differences in encapsulation energies are due to different estimations of the electronic nature of the complexes by different functionals. The encapsulation energy found for the ^{1}(B@2) complex obtained at DLPNO-CCSD(T)/cc-PVTZ//PBE0/6-311+G(2d) was −65.85 kcal mol^{-1}. The encapsulation energies obtained for the same geometries with the PBE0 and B3LYP functionals were −52.11 and −36.90 kcal mol^{-1} respectively.

Taking into account also the slightly better performance of the PBE0 functional towards ionization potential predictions for individual FLi_2 and B_{39} subunits, as well as the apparently more reliable description of the stabilization energies for the supermolecules of interest, we have decided to use only the PBE0 functional for further calculations. Table 1 demonstrates the energies of encapsulation ($\Delta E_{encap.}$), deformation energies ($\Delta E_{def.}$) and interaction energies ($\Delta E_{int.}$) for the ^{3}(A@1), ^{2}(B@1)$^+$, ^{2}(A@2)$^-$ and ^{1}(B@2) supermolecules obtained at the PBE0/6-311+G(2d) level of theory. The detailed description of the $\Delta E_{encap.}$, $\Delta E_{def.}$, and $\Delta E_{int.}$ calculation methods as well as fragment determination are presented in Scheme S1 and in eqn (E.1)–(E.4) and (D.1)–(D.4) of the ESI.†

Only ^{2}(B@1)$^+$ complex formation is a thermodynamically unfavorable process. In all other cases, the formation of the complexes is clearly an exothermic process. As could be seen in

Table 1 Encapsulation ($\Delta E_{encap.}$), interaction ($\Delta E_{int.}$), and deformation ($\Delta E_{def.}$) energies calculated for the studied supermolecules as well as for their fragments[a] ($\Delta E^{F1}_{def.}$ and $\Delta E^{F2}_{def.}$) obtained at the PBE0/6-311+g(2d) level of theory

	^{3}(A@1)	^{2}(B@1)$^+$	^{2}(A@2)$^-$	^{1}(B@2)
$\Delta E_{encap.}$	−10.23	23.70	−10.66	−52.11
$\Delta E^{F1}_{def.}$	9.35	7.81	12.34	7.69
$\Delta E^{F2}_{def.}$	1.43	18.09	1.39	17.57
$\Delta E^{total}_{def.}$	10.78	25.90	13.74	25.26
$\Delta E_{int.}$	−21.01	−2.20	−24.40	−77.36

[a] F1 is $B_{39}^{0/1-}$ species, F2 is $FLi_2^{0/1+}$ species. The detailed decomposition scheme is shown in Scheme S1, ESI. $\Delta E_{encap.} = \Delta E_{def.} + \Delta E_{int.}$.

Table S5 (ESI†), the encapsulation process causes substantial shortening of the F–Li bond by 0.06 to 0.07 Å in all cases. However, when cationic FLi_2 is used as the encapsulation object (^{2}(B@1)$^+$ and ^{1}(B@2) systems), significant changes in the Li–F–Li valence angle are observed. Taking into account that such changes amount to the order of about 70 degrees we can determine that in such supermolecules the FLi_2 fragment is significantly strained as confirmed by the high values of deformation energies ($\Delta E^{F2}_{def.}$) of the discussed fragment in the ^{2}(B@1)$^+$ and ^{1}(B@2) structures compared with the ^{3}(A@1) and ^{2}(A@2)$^-$ ones (see Table 1). The energies of deformation for the B_{39} species (fragment 1) slightly differ from system to system, but generally are comparable. Slightly larger values may be noted for the ^{3}(A@1) and ^{2}(A@2)$^-$ systems. At the same time, the ^{1}(B@2) cluster demonstrates the highest value of the interaction energy among all studied complexes. Considering the fact that the ^{1}(B@2) complex is formed by the cationic FLi_2 species and B_{39} anion, we can assume that the high interaction energy is provided basically by electrostatic attraction. This also explains why in all other cases the interaction energies are noticeably weaker. It is worth noting that if we consider $LiF_2@B_{39}$ formed from LiF_2 and B_{39}, then the encapsulation energy of LiF_2 into B_{39} is −45.90 kcal mol^{-1}. Thus, homolytic separation of $LiF_2@B_{39}$ into LiF_2 and B_{39} fragments is slightly more favorable than the heterolytic one into LiF_2^+ and B_{39}^- by 6.21 kcal mol^{-1}.

The ^{3}(A@1) and ^{2}(A@2)$^-$ complexes are characterized by significant interaction energies and are thermodynamically favorable. Both of these complexes comprise FLi_2 species containing one unpaired electron. In order to determine an actual charge and spin density distribution (Table S6, ESI†), the natural population analysis scheme for each complex at equilibrium geometry has been applied. Our results show that the formation of complexes ^{3}(A@1) and ^{2}(A@2)$^-$ is associated with unpaired electron transfer from the FLi_2 fragment to the B_{39} cage. Thus, taking into account that almost all spin density in these complexes is localized on the cage, ^{3}(A@1) and ^{2}(A@2)$^-$ could be formally represented with the formulas $LiF_2^+@B_{39}^{1-}$ and $LiF_2^+@B_{39}^{2-}$, respectively. On one hand, a driving force for the designated electron transfer is the significantly better electron delocalization ability of B_{39} species. On the other hand, the extremely low IP of FLi_2 favors the charge transfer. An additional factor of stabilization in the ^{2}(A@2)$^-$ complex is the charge-induced dipole interaction between FLi_2 and B_{39}^-.

The above-mentioned stabilization factors, except charge-induced dipole interaction, are not observed in the case of the $^{2}(B@1)^{+}$ complex with small interaction energy. This fact as well as the remarkable deformation energy for the FLi_2 fragment lead to the result that $^{2}(B@1)^{+}$ complex formation is endothermic and a thermodynamically unfavorable process.

The encapsulation energy analysis based on Gibbs energies at 298 K has been performed as well. $\Delta E_{encap.}^{Gibbs}$ was found to be +3.54, +38.86, +3.21 and −36.88 for $^{3}(A@1)$, $^{2}(B@1)^{+}$, $^{2}(A@2)^{-}$ and $^{1}(B@2)$, respectively. It has to be noted that the complex stabilization energies estimated *via* Gibbs energies in all studied cases are approximately 14 to 15 kcal mol^{-1} less than the estimations obtained with electronic energies.

The ionization process of an atom or a molecule from an energetic point of view can be described in several ways using adiabatic and non-adiabatic (vertical) formalisms. The adiabatic ionization energy (AIP) is the minimum amount of energy required to remove an electron from a neutral atom or molecule. Subsequently, adiabatic electron affinity (AEA) is the amount of energy released when an electron is added to a neutral atom or molecule. In other words, AIP and AEA are the difference between the ground state energy of neutral species and that of a positively or negatively charged ion. On the other hand, vertically determined potentials can be divided into two groups depending on the point of reference. If we define energy difference between the neutral molecule and its negative or positively charged ion, both of which are in their initial (neutral molecule) geometry, in this case the designated energy differences are vertical electron affinity (VEA) and vertical ionization potential (VIP), respectively. However, if the negatively or positively charged ion has been selected as the reference point, then such energy differences between the denoted ion and neutral molecule in the ion initial geometry are vertical detachment energy (VDE) and vertical attachment energy (VAE), respectively (see Fig. 3).

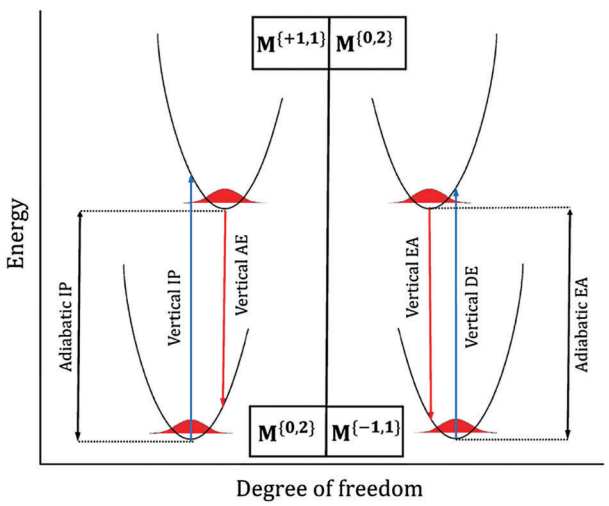

Fig. 3 Schematic diagrams illustrating the terms of electron affinity (EA), ionization potential (IP), vertical EA, and vertical IP as well as vertical detachment and attachment energies for molecules with hypothetical Born–Oppenheimer potential energy surfaces.

Table 2 Computationally obtained values of adiabatic IP and EA, and vertical IP, AE, EA, and DE energies for B_{39} and FLi_2 species as well as for the $^{1}(B@2)$ ($FLi_2@B_{39}$) endohedral complex

Molecule	AIP, eV	VIP, eV	VAE, eV	AEA, eV	VEA, eV	VDE, eV
$^{1}(B@2)$	7.19	7.34	6.99	2.38	2.20	2.54
B_{39} {0,2}	—	—	—	3.90	3.77	4.03
FLi_2 {0,2}	4.17	4.86	4.04	—	—	—

If we consider the vertical potential as some approximation of the adiabatic one it should be noted that VIP always will somehow overestimate the adiabatic values, while VAE will underestimate the values of adiabatic IP to a certain degree. In the case of electron affinity, the situation is reversed – VDE will overestimate the adiabatic EA, while VEA will underestimate it. The non-equivalence of the vertical and adiabatic values is due to the changes in the geometry of species of reference during the ionization process. Obviously, the use of vertical potentials in computational chemistry is often more convenient because it allows one to avoid calculations for systems with an open-shell electron configuration and related difficulties. On the other hand, experimentally used methods for IP or EA determination frequently provide values associated with vertical processes. In our work, we systematically compare adiabatic and vertical ionization energies and electron affinities as well as vertical attachment and detachment energies for the $^{1}(B@2)$ supermolecule and fragments (B_{39} and FLi_2) of which it is composed (Table 2).

The obtained ionization energies and electron affinities demonstrate that the $FLi_2@B_{39}$ endohedral system loses both SA and SH properties inherent in the individual subunits. At the same time, it should be noted that calculated potentials behave in full accordance with our expectations. We have shown that for the systems investigated here, vertical potentials can be efficiently utilized as a good approximation for subsequent adiabatic potentials in endohedral systems similar to those studied in this work. For instance, for the $^{1}(B@2)$ system the absolute error for both adiabatic IP and EA in comparison with vertically defined values never exceeds 0.2 eV, *i.e.* a few percent in a relative scale (Table S7, ESI†). The results are very similar to the case of the B_{39} fragment. However, it should be stressed that the inaccuracy of adiabatic IP and EA can substantially increase simultaneously with decreasing the molecular system size. As can be seen from Table S7 (ESI†), the relative difference between vertical and adiabatic IP values for FLi_2 species can reach a noticeable 16%, or as an absolute value it is about 0.7 eV.

Conclusions

In conclusion, we have predicted and presented at the PBE0/6-311+G(2d) level the viability of the first endohedral $FLi_2@B_{39}$ borospherene family composed of superalkaline and superhalogen fragments or/and their conjugated ions. All studied endohedral borospherenes, except the $^{2}(B@1)^{-}$ system, demonstrate thermodynamic stability caused most likely by electrostatic attraction and unpaired electron delocalization. Based on

the studies of adiabatic ionization potential and electron affinity for the $FLi_2@B_{39}$ borospherenes, we found that the denoted systems lose their "super" properties. In addition, we demonstrated that easily available vertically estimated potentials could be used for approximation of adiabatic values for endohedral borospherenes. We hope that the findings presented in this work will not only enrich our knowledge on superatom chemistry and the electronic properties of encapsulated borospherenes, but also stimulate interest in further research by both theoretical scientists and experimentalists in the field of materials science.

Acknowledgements

The authors acknowledge the support of the Ministerio de Economía y Competitividad of Spain (Project CTQ2014-54306-P), Generalitat de Catalunya (project number 2014SGR931, Xarxa de Referència en Química Teòrica i Computacional, and ICREA Academia prize 2014 for MS), and the European Fund for Regional Development (FEDER grant UNGI10-4E-801). A. J. S. gratefully acknowledges The Interdisciplinary Centre for Mathematical and Molecular Modelling of the University of Warsaw (ICM) for computational facilities (grant no. G-3317). The authors thank Dr D. Sharapa for logistical help.

Notes and references

1 G. L. Gutsev and A. I. Boldyrev, *Chem. Phys. Lett.*, 1982, **92**, 262–266.
2 G. L. Gutsev and A. I. Boldyrev, *Zh. Neorg. Khim.*, 1983, **28**, 2179–2181.
3 G. L. Gutsev and A. I. Boldyrev, *Chem. Phys. Lett.*, 1981, **84**, 352–355.
4 G. L. Gutsev and A. I. Boldyrev, *Chem. Phys.*, 1981, **56**, 277–283.
5 M. A. Lennon, K. L. Bell, H. B. Gilbody, J. G. Hughes, A. E. Kingston, M. J. Murray and F. J. Smith, *J. Phys. Chem. Ref. Data*, 1988, **17**, 1285–1363.
6 R. E. Leuchtner, A. C. Harms and A. W. Castleman Jr., *J. Chem. Phys.*, 1989, **91**, 2753–2754.
7 P. Jena, S. N. Khanna and B. K. Rao, *Surf. Rev. Lett.*, 1996, **03**, 993–999.
8 P. Jena, *J. Phys. Chem. Lett.*, 2013, **4**, 1432–1442.
9 Z. Luo and A. W. Castleman, *Acc. Chem. Res.*, 2014, **47**, 2931–2940.
10 A. C. Reber and S. N. Khanna, *Acc. Chem. Res.*, 2017, **50**, 255–263.
11 A. K. Srivastava and N. Misra, *RSC Adv.*, 2015, **5**, 74206–74211.
12 J. Tong, Y. Li, D. Wu and Z. J. Wu, *Inorg. Chem.*, 2012, **51**, 6081–6088.
13 E. Zurek, *J. Am. Chem. Soc.*, 2011, **133**, 4829–4839.
14 J. Tong, Y. Li, D. Wu, Z. R. Li and X. R. Huang, *J. Chem. Phys.*, 2009, **131**, 164307.
15 B. Q. Wang, Z. R. Li, D. Wu and F. F. Wang, *J. Phys. Chem. A*, 2007, **111**, 6378–6382.
16 H. Kudo, *J. Nucl. Radiochem. Sci.*, 2001, **2**, R13–R21.
17 C. H. Wu, H. Kudoa and H. R. Ihle, *J. Chem. Phys.*, 1979, **70**, 1815–1820.
18 T. J. Carter, R. Mohtadi, T. S. Arthur, F. Mizuno, R. Zhang, S. Shirai and J. W. Kampf, *Angew. Chem., Int. Ed.*, 2014, **53**, 3173–3177.
19 L. Cheng, Y. Yuan, X. Zhang and J. Yang, *Angew. Chem., Int. Ed.*, 2013, **52**, 9035–9039.
20 C. H. Wu, *Chem. Phys. Lett.*, 1987, **139**, 357–359.
21 P. v. R. Schleyer, E. U. Wuerthwein and J. A. Pople, *J. Am. Chem. Soc.*, 1982, **104**, 5839–5841.
22 F. M. Veljkovic, J. B. Djustebek, M. V. Veljkovic, S. R. Velickovic and A. A. Peric-Grujic, *Rapid Commun. Mass Spectrom.*, 2012, **26**, 1761–1766.
23 S. R. Velickovic, J. B. Djustebek, F. M. Veljkovic, B. B. Radak and M. V. Veljkovic, *Rapid Commun. Mass Spectrom.*, 2012, **26**, 443–448.
24 A. K. Srivastava and N. Misra, *New J. Chem.*, 2015, **39**, 6787–6790.
25 A. K. Srivastava and N. Misra, *J. Mol. Model.*, 2015, **21**, 305.
26 I. Anusiewicz, *Aust. J. Chem.*, 2010, **63**, 1573–1581.
27 F.-F. Wang, Z.-R. Li, D. Wu, X.-Y. Sun, W. Chen, Y. Li and C.-C. Sun, *ChemPhysChem*, 2006, **7**, 1136–1141.
28 H. Fang and P. Jena, *J. Phys. Chem. Lett.*, 2016, **7**, 1596–1603.
29 H. Zhao, J. Zhou, H. Fang and P. Jena, *ChemPhysChem*, 2016, **17**, 184–189.
30 M. Czapla and P. Skurski, *J. Phys. Chem. A*, 2015, **119**, 12868–12875.
31 Y. Li, D. Wu and Z.-R. Li, *Inorg. Chem.*, 2008, **47**, 9773–9778.
32 S.-J. Wang, Y. Li, Y.-F. Wang, D. Wu and Z.-R. Li, *Phys. Chem. Chem. Phys.*, 2013, **15**, 12903–12910.
33 C. Paduani, *Phys. E*, 2016, **77**, 199–205.
34 T. Zhao, S. Zhang, Q. Wang, Y. Kawazoe and P. Jena, *Phys. Chem. Chem. Phys.*, 2014, **16**, 22979–22986.
35 B. Yin, J. Li, H. Bai, Z. Wen, Z. Jiang and Y. Huang, *Phys. Chem. Chem. Phys.*, 2012, **14**, 1121–1130.
36 M. M. Wu, H. Wang, Y. J. Ko, Q. Wang, Q. Sun, B. Kiran, A. K. Kandalam, K. H. Bowen and P. Jena, *Angew. Chem., Int. Ed.*, 2011, **50**, 2568–2572.
37 P. Jena, *J. Phys. Chem. Lett.*, 2015, **6**, 1119–1125.
38 S. Giri, S. Behera and P. Jena, *Angew. Chem., Int. Ed.*, 2014, **53**, 13916–13919.
39 L.-J. Zhao, H.-G. Xu, G. Feng, P. Wang, X.-L. Xu and W.-J. Zheng, *Phys. Chem. Chem. Phys.*, 2016, **18**, 6175–6181.
40 J.-F. Li, Y.-Y. Sun, H. Bai, M.-M. Li, J.-L. Li and B. Yin, *AIP Adv.*, 2015, **5**, 067143.
41 J.-F. Li, M.-M. Li, H. Bai, Y.-Y. Sun, J.-L. Li and B. Yin, *ChemPhysChem*, 2015, **16**, 3652–3659.
42 H.-J. Zhai, Y.-F. Zhao, W.-L. Li, Q. Chen, H. Bai, H.-S. Hu, Z. A. Piazza, W.-J. Tian, H.-G. Lu, Y.-B. Wu, Y.-W. Mu, G.-F. Wei, Z.-P. Liu, J. Li, S.-D. Li and L.-S. Wang, *Nat. Chem.*, 2014, **6**, 727–731.
43 Q. Chen, W.-L. Li, Y.-F. Zhao, S.-Y. Zhang, H.-S. Hu, H. Bai, H.-R. Li, W.-J. Tian, H.-G. Lu, H.-J. Zhai, S.-D. Li, J. Li and L.-S. Wang, *ACS Nano*, 2015, **9**, 754–760.

44 Q. Chen, S.-Y. Zhang, H. Bai, W.-J. Tian, T. Gao, H.-R. Li, C.-Q. Miao, Y.-W. Mu, H.-G. Lu, H.-J. Zhai and S.-D. Li, *Angew. Chem., Int. Ed.*, 2015, **54**, 8160–8164.
45 R. He and X. C. Zeng, *Chem. Commun.*, 2015, **51**, 3185–3188.
46 S. Li, Z. Zhang, Z. Long, G. Sun and S. Qin, *Sci. Rep.*, 2016, **6**, 25020.
47 Y.-J. Wang, Y.-F. Zhao, W.-L. Li, T. Jian, Q. Chen, X.-R. You, T. Ou, X.-Y. Zhao, H.-J. Zhai, S.-D. Li, J. Li and L.-S. Wang, *J. Chem. Phys.*, 2016, **144**, 064307.
48 J. R. Heath, S. C. O'Brien, Q. Zhang, Y. Liu, R. F. Curl, F. K. Tittel and R. E. Smalley, *J. Am. Chem. Soc.*, 1985, **107**, 7779–7780.
49 Y. Chai, T. Guo, C. Jin, R. E. Haufler, L. P. F. Chibante, J. Fure, L. Wang, J. M. Alford and R. E. Smalley, *J. Phys. Chem.*, 1991, **95**, 7564–7568.
50 R. C. Haddon, A. F. Hebard, M. J. Rosseinsky, D. W. Murphy, S. J. Duclos, K. B. Lyons, B. Miller, J. M. Rosamilia, R. M. Fleming, A. R. Kortan, S. H. Glarum, A. V. Makhija, A. J. Muller, R. H. Eick, S. M. Zahurak, R. Tycko, G. Dabbagh and F. A. Thiel, *Nature*, 1991, **350**, 320–322.
51 H. Bai, Q. Chen, H.-J. Zhai and S.-D. Li, *Angew. Chem., Int. Ed.*, 2015, **54**, 941–945.
52 G. Martinez-Guajardo, J. L. Cabellos, A. Diaz-Celaya, S. Pan, R. Islas, P. K. Chattaraj, T. Heine and G. Merino, *Sci. Rep.*, 2015, **5**, 11287.
53 Q. Chen, T. Gao, W.-J. Tian, H. Bai, S.-Y. Zhang, H.-R. Li, C.-Q. Miao, Y.-W. Mu, H.-G. Lu, H.-J. Zhai and S.-D. Li, *Phys. Chem. Chem. Phys.*, 2015, **17**, 19690–19694.
54 Q. Chen, H. R. Li, W. J. Tian, H. G. Lu, H. J. Zhai and S. D. Li, *Phys. Chem. Chem. Phys.*, 2016, **18**, 14186–14190.
55 Q. Chen, H.-R. Li, C.-Q. Miao, Y.-J. Wang, H.-G. Lu, Y.-W. Mu, G.-M. Ren, H.-J. Zhai and S.-D. Li, *Phys. Chem. Chem. Phys.*, 2016, **18**, 11610–11615.
56 H. Bai, B. Bai, L. Zhang, W. Huang, Y.-W. Mu, H.-J. Zhai and S.-D. Li, *Sci. Rep.*, 2016, **6**, 35518.
57 A. K. Srivastava, S. K. Pandey and N. Misra, *Chem. Phys. Lett.*, 2016, **656**, 71–75.
58 K. Komatsu, M. Murata and Y. Murata, *Science*, 2005, **307**, 238–240.
59 A. Krachmalnicoff, M. H. Levitt and R. J. Whitby, *Chem. Commun.*, 2014, **50**, 13037–13040.
60 K. Kurotobi and Y. Murata, *Science*, 2011, **333**, 613–616.
61 E. E. Maroto, J. Mateos, M. Garcia-Borràs, S. Osuna, S. Filippone, M. A. Herranz, Y. Murata, M. Solà and N. Martín, *J. Am. Chem. Soc.*, 2015, **137**, 1190–1197.
62 A. Krachmalnicoff, R. Bounds, S. Mamone, S. Alom, M. Concistrè, B. Meier, K. Kouřil, M. E. Light, M. R. Johnson, S. Rols, A. J. Horsewill, A. Shugai, U. Nagel, T. Rõõm, M. Carravetta, M. H. Levitt and R. J. Whitby, *Nat. Chem.*, 2016, **8**, 953–957.
63 S. Giri, S. Behera and P. Jena, *J. Phys. Chem. A*, 2014, **118**, 638–645.
64 A. K. Srivastava and N. Misra, *Mol. Phys.*, 2014, **112**, 2621–2626.
65 A. K. Srivastava and N. Misra, *New J. Chem.*, 2014, **38**, 2890–2893.
66 K. Yokoyama, N. Haketa, H. Tanaka, K. Furukawa and H. Kudo, *Chem. Phys. Lett.*, 2000, **330**, 339–346.
67 O. M. Nešković, M. V. Veljković, S. R. Veličković, L. T. Petkovska and A. A. Perić-Grujić, *Rapid Commun. Mass Spectrom.*, 2003, **17**, 212–214.
68 A. K. Srivastava and N. Misra, *J. Mol. Model.*, 2015, **21**, 147.
69 J. Tao, J. P. Perdew, V. N. Staroverov and G. E. Scuseria, *Phys. Rev. Lett.*, 2003, **91**, 146401.
70 V. N. Staroverov, G. E. Scuseria, J. Tao and J. P. Perdew, *J. Chem. Phys.*, 2003, **119**, 12129–12137.
71 C. Adamo and V. Barone, *J. Chem. Phys.*, 1998, **108**, 664–675.
72 J. Heyd and G. E. Scuseria, *J. Chem. Phys.*, 2004, **120**, 7274–7280.
73 J. Heyd and G. E. Scuseria, *J. Chem. Phys.*, 2004, **121**, 1187–1192.